

Accuracy measurement of an at-home refraction measurement device

Noam Sapiens^{✉*} and Patrick O'Neal

EyeQue Corporation, Newark, California, United States

Abstract. An investigation of the accuracy and reproducibility of refraction measurements of an at-home refraction measurement device is carried in a standardized experimental setup. The refraction measurement device is a handheld, low-cost, and simple to use refraction measurement device based on the inverse Shack–Hartmann technology. The device is aimed for consumers, telehealth, and at-home measurements. Users attach the device to their smartphone for control and analysis of the measurement. Looking through the device, users align patterns from the screen through two separated optical channels. The patterns combine on the user's retina depending on their refraction values. A derivation of the formulation of the method is presented. The results of the accuracy assessment are analyzed through linear regression showing very good match between the input refraction values and the measured ones. Reproducibility result also show low variation between devices. © The Authors. Published by SPIE under a Creative Commons Attribution 4.0 International License. Distribution or reproduction of this work in whole or in part requires full attribution of the original publication, including its DOI. [DOI: [10.1117/1.OE.61.12.121805](https://doi.org/10.1117/1.OE.61.12.121805)]

Keywords: refraction; telehealth; Shack–Hartmann; ophthalmic.

Paper 20220575SS received May 31, 2022; accepted for publication Sep. 19, 2022; published online Oct. 14, 2022.

1 Introduction

Uncorrected refractive error is the most prevalent eye condition globally. It accounts for more than 40% of the major causes for visual impairment.^{1,2} Refraction measurement is one of the most commonly performed procedures done by eye care professionals. It is used to diagnose, monitor, or plan treatment of a variety of conditions. These include myopia, hyperopia, astigmatism, presbyopia, and other diseases and conditions that affect refractive error. Ophthalmic refraction measurements are traditionally performed by eye care professionals using devices such as autorefractors and phoropters. These devices for refraction measurements are cumbersome, expensive, and require professional training for their operation. Demand for telehealth and remote services by patients and healthcare providers has accelerated the development of new technologies to improve access and lower the cost of care.^{3–5} The COVID-19 pandemic magnified this trend for telemedicine.^{6–8} Eye care has similarly produced such advancements allowing handheld, low-cost, and simple to use devices to elevate standard of care by allowing users to perform self-administered measurements in the comfort of their home, outside of the clinic. The EyeQue VisionCheck is a self-administered, mobile application-driven refraction measurement device that provides spherical, cylindrical, and axis correction metrics of the eye. We turn to assess this device's accuracy in a laboratory setup under its expected operating conditions.

1.1 Measurement Device Operation

The EyeQue VisionCheck device is a lightweight, rechargeable device that attaches to a smartphone running the EyeQue VisionCheck App. The smartphone screen acts as the light source. Two lines are presented on the screen and light from each line passes through each of two optical channels of the device. The separation of the lines on the screen is correlated to refractive power and is adjusted by the user. To measure an eye's refractive power in terms of sphere, cylinder, and

*Address all correspondence to Noam Sapiens, noam.sapiens@eyeque.com

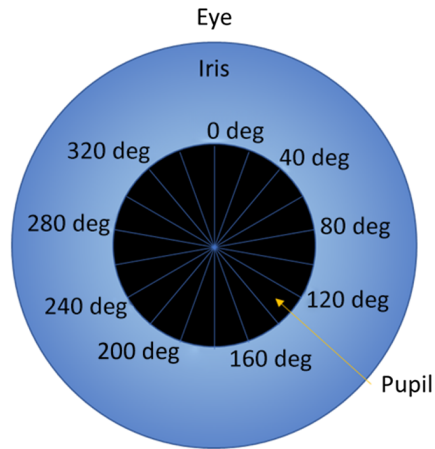


Fig. 1 A schematic representation of the measurement meridians on the pupil.



Fig. 2 EyeQue VisionCheck device (shown as attached to a smartphone).

axis, mapping of the eye is made through measurements at different meridians around the pupil. The device includes rotation of the optical channels around the optical axis that is used to make diopter power measurements at different meridians. The device uses nine meridians, separated by 40 deg, as shown in Fig. 1.

The smartphone application guides the user through the refraction test. The user looks through the eyepiece at a test pattern consisting of one red line and one green line presented by the smartphone application. On top of the device are three buttons: two that control moving the red and green lines closer/farther apart, and one that advances to the next measurement. Figure 2 shows the EyeQue VisionCheck device attached to a smartphone.

The user presses the buttons bringing the lines closer together until they overlap and form a single yellow line, as shown in Fig. 3. The perception of the overlapped lines occurs when the

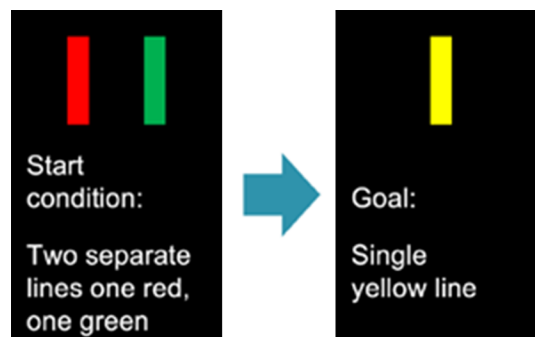


Fig. 3 A schematic representation of the red and green lines seen through the device at the beginning of a measurement and the overlap alignment to a single yellow line.

light from the lines converges on the retina. The distance between the lines on the screen when the user perceives them overlapped is used to calculate the refractive power for the given meridian.

1.2 Inverse Shack–Hartmann Technology

A traditional Shack–Hartmann measurement is comprised of segmentation of the input beam into multiple channels using an array of lenses or apertures. The deviation of the foci from the prospective optical axes of each of the channels of the array elements gives indication of the angle/phase of each individual channel. The inverse Shack–Hartmann technology^{9–11} is based on the same principle, only the input beam is modified such that the foci for each channel is set to the same optical axis. The original beam phase/angle at each channel is then proportional to the required change in the beam.

The use of the inverse Shack–Hartmann principle to refraction measurement of the human eye relies on input from the user related to the required deviation. The user makes changes to the input beam to align the foci onto the optical axis of the system. To simplify the cognitive load of such a measurement, the refraction measurement of the human eye relies on only two channels per measurement. Multiple measurements at different meridians are used to increase the aberration order that could be measured and reduce the inherent noise in the measurement. Measuring more meridians increases the amount of information regarding the optical system aberrations. Furthermore, this increase in the number of data points could be used to reduce noise in the system by different algorithms, e.g., averaging, fitting, and smoothing. A refraction measurement based on the inverse Shack–Hartman principle is composed of an input beam based on a light source able to present patterns to the user (e.g., screen), an optical system that relays the patterns through to separate optical channels, the optical prospect of the eye and the retina—used to determine the alignment of the patterns. The change in the input beam is performed by adjusting the pattern on the screen. The optical measurement system allows the adjustment to be made for different meridians of the optical channels with relation to the measured optical system, the eye. As light emanates from the screen and traverses through two separate channels of the measurement device, the position of the lines on the screen with respect to the device optical axis is converted to an angle at the output. Figure 4 shows the governing principle of inverse Shack–Hartmann devices spatial to angular conversion.

This conversion function is a characteristic of the measurement device. The angle originating from the device then enters the eye and is converted back to spatial information on the retina. The power of the eye determines which angle would constitute an overlap of the signals from the two separate channels in the device.

The range of the angle α for a range of human refraction correction between -10 D and $+8$ D is (-1.77 deg, 1.79 deg). The paraxial approximation will therefore be utilized throughout the paper. Figure 5 shows a schematic model used in the formulation.

The analysis follows a point (x, y) on the screen in its transformation onto the retina. Begin with the transfer of the point from the screen through the optical system. Figure 6 shows a representation of the associated coordinate systems.

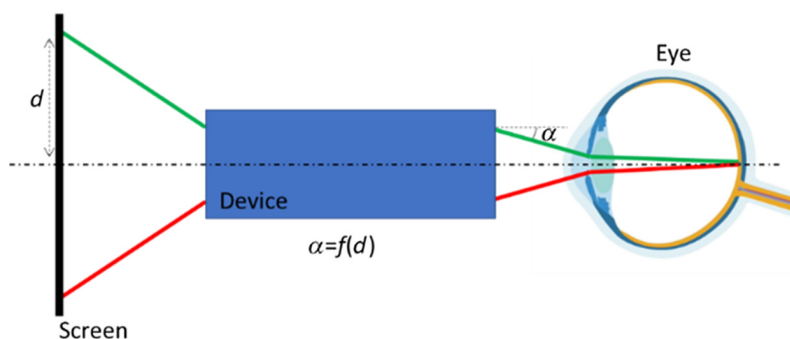


Fig. 4 Conversion of screen pattern position to output angle in inverse Shack–Hartmann devices.

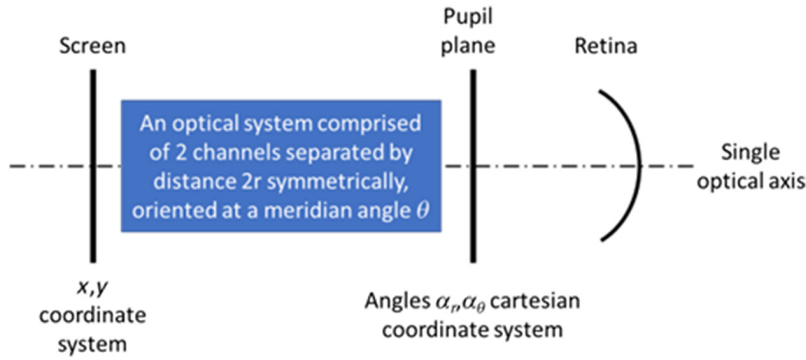


Fig. 5 Model schematics.

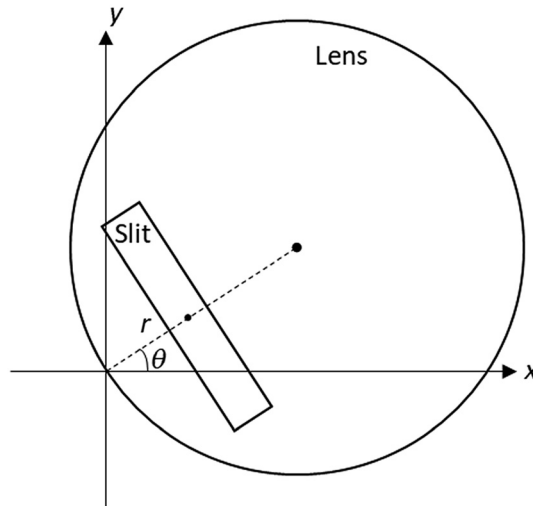


Fig. 6 Coordinate system through the device optics.

Light emerges from the measurement device at the same location regardless of the output angle. The output angle is the parameter that is changing and it depends on the coordinates (x, y) of the pattern on the screen, the distance between the channels $2r$, and the meridian angle θ .

Define coordinates x_m, y_m rotated by an angle θ to the x, y axes:

$$x_m = x \cos(\theta) + y \sin(\theta), \tag{1}$$

$$y_m = y \cos(\theta) - x \sin(\theta). \tag{2}$$

In the (x_m, y_m) coordinate system, an example of an optical design of an inverse Shack–Hartmann device (EyeQue VisionCheck) is shown in Fig. 7.

Using the ray transfer matrix method, we can find the output from the input. For the radial axis, Eq. (3) presents the ray propagation through the system

$$\begin{pmatrix} 1 & z_3 \\ 0 & 1 \end{pmatrix} \begin{pmatrix} 1 & 0 \\ -1/f_2 & 1 \end{pmatrix} \Big|_a \begin{pmatrix} 1 & z_2 \\ 0 & 1 \end{pmatrix} \begin{pmatrix} 1 & 0 \\ -1/f_1 & 1 \end{pmatrix} \begin{pmatrix} 1 & z_1 \\ 0 & 1 \end{pmatrix} \begin{pmatrix} x_m \\ \beta_x \end{pmatrix} = \begin{pmatrix} x_m + \beta_x(z_1 + z_2 + z_3) - \frac{z_2 + z_3}{f_1}(x_m + \beta_x z_1) - \frac{z_3}{f_2}[x_m + \beta_x(z_1 + z_2)] - \frac{z_2}{f_1}(x_m + \beta_x z_1) - a \\ \beta_x - \frac{x_m + \beta_x z_1}{f_1} - \frac{1}{f_2}[x_m + \beta_x(z_1 + z_2)] - \frac{z_2}{f_1}(x_m + \beta_x z_1) - a \end{pmatrix}. \tag{3}$$

Since the ray position is defined by the channel as r , we can find β_x by solving Eq. (4)

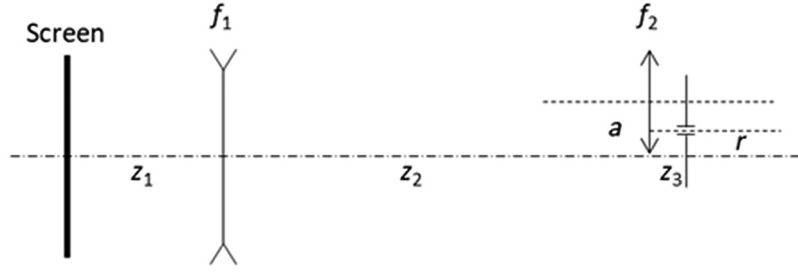


Fig. 7 EyeQue VisionCheck single-channel geometrical optical design. Where z_1 is the distance on the optical axis from the screen to lens f_1 , f_1 is the focal length of the negative lens, z_2 is the distance between the f_1 and the f_2 lenses, a is the radial offset of the center of the f_2 lens, f_2 is the focal length of the positive lens, z_3 is the distance between the f_2 lens and the aperture, and r is the radial offset of the center of the aperture.

$$x_m + \beta_x(z_1 + z_2 + z_3) - \frac{z_2 + z_3}{f_1}(x_m + \beta_x z_1) - \frac{z_3}{f_2} \left[x_m + \beta_x(z_1 + z_2) - \frac{z_2}{f_1}(x_m + \beta_x z_1) - a \right] = r. \quad (4)$$

Marking:

$$U = 1 - \frac{z_2 + z_3}{f_1} - \frac{z_3}{f_2} + \frac{z_2 z_3}{f_1 f_2}, \quad (5)$$

$$V = r - \frac{z_3 a}{f_2}, \quad (6)$$

$$Q = z_1 + z_2 + z_3 - \frac{z_1(z_2 + z_3)}{f_1} - \frac{z_3(z_1 + z_2)}{f_2} + \frac{z_1 z_2 z_3}{f_1 f_2}. \quad (7)$$

We find:

$$\beta_x = \frac{V}{Q} - \frac{U}{Q} x_m. \quad (8)$$

Since traversing the center of the channel in the tangential direction does not introduce any angular shifts (this is due to the fact that it can be treated as going through the center of a lens in that direction and that a spherical lens like f_2 directs light in a radial direction), the treatment for the tangential direction may assume $f_2 \rightarrow \infty$. Thus getting:

$$\beta_y = \frac{V}{Q} - \frac{U}{Q} y_m \Big|_{f_2 \rightarrow \infty}. \quad (9)$$

The output angles may now be calculated as

$$\alpha_r = \beta_x - \frac{x_m + \beta_x z_1}{f_1} - \frac{1}{f_2} \left[x_m + \beta_x(z_1 + z_2) - \frac{z_2}{f_1}(x_m + \beta_x z_1) - a \right], \quad (10)$$

$$\alpha_\theta = \beta_y - \frac{y_m + \beta_y z_1}{f_1}. \quad (11)$$

These are independent linear expressions of x_m, y_m or dependent linear expressions of x, y .

From here on out α_r, α_θ will be used as the local coordinate system. For meridian θ , the coordinate system of the incidence angles on the pupil plane is rotated such that there is a radial axis and a tangential axis. These axes are orthogonal and are defined in Fig. 8, where the distance between the channel output and the pupil plane is neglected as a good approximation for the sake

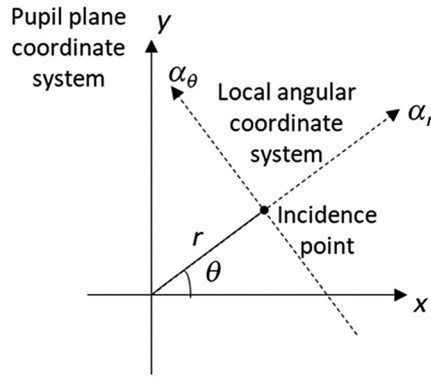


Fig. 8 Pupil plane coordinate systems.

of simplicity in this analysis. In reality, this distance exists and introduces a slight deviation from the presented position and orientation of these axes. This deviation is captured in real systems as part of the system calibration.

The pupil plane could be modeled as an angular offset screen described by a field of the form $\bar{\Psi} \begin{pmatrix} \Psi_r(r, \theta) \\ \Psi_\theta(r, \theta) \end{pmatrix}$ such that the angles after the screen are $\begin{pmatrix} \alpha_r + \Psi_r(r, \theta) \\ \alpha_\theta + \Psi_\theta(r, \theta) \end{pmatrix}$.

Starting with a few example cases, we derive the screen formulation for a spherical lens and a cylindrical lens.

For a spherical lens of power S , based on the ray transfer matrix method, we find that the angles after the screen will be:

$$\begin{pmatrix} \alpha_r - Sr \\ \alpha_\theta \end{pmatrix}, \tag{12}$$

which indicates that for a paraxial infinite spherical lens with optical axis coinciding with the z axis the angle offset field is

$$\bar{\Psi} = \begin{pmatrix} -Sr \\ 0 \end{pmatrix}. \tag{13}$$

The case of a paraxial infinite pure cylindrical lens with optical axis coinciding with the z axis is shown in Fig. 9.

Since this case is not centrosymmetric, the two-dimensional ray transfer matrix method used is inappropriate. A more inclusive method is used based on a four-dimensional ray transfer matrix. In this case, the input vector has four elements signifying the positions and angles in two orthogonal directions. The transfer matrix is a 4×4 linear transformation matrix. As such,

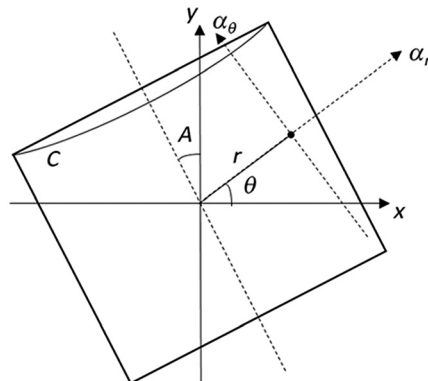


Fig. 9 Pure cylindrical lens.

rotation of the axes could be computed through multiplication with a rotation matrix in the form: $R(-A) \cdot C \cdot R(A)$ where $R(A)$ is a rotation matrix by an angle A of the form:

$$R(A) = \begin{pmatrix} \cos(A) & 0 & \sin(A) & 0 \\ 0 & \cos(A) & 0 & \sin(A) \\ -\sin(A) & 0 & \cos(A) & 0 \\ 0 & -\sin(A) & 0 & \cos(A) \end{pmatrix}. \quad (14)$$

C is the matrix for rotating, in our case, a cylindrical lens matrix:

$$C = \begin{pmatrix} 1 & 0 & 0 & 0 \\ -C & 1 & 0 & 0 \\ 0 & 0 & 1 & 0 \\ 0 & 0 & 0 & 1 \end{pmatrix}. \quad (15)$$

In our case, the output vector becomes:

$$\begin{pmatrix} 1 & 0 & 0 & 0 \\ -C \sin^2(\theta - A) & 1 & -C \sin(\theta - A) \cos(\theta - A) & 0 \\ 0 & 0 & 1 & 0 \\ -C \sin(\theta - A) \cos(\theta - A) & 0 & -C \cos^2(\theta - A) & 1 \end{pmatrix} \begin{pmatrix} r \\ \alpha_r \\ 0 \\ \alpha_\theta \end{pmatrix} \\ = \begin{pmatrix} r \\ \alpha_r - Cr \sin^2(\theta - A) \\ 0 \\ \alpha_\theta - Cr \sin(\theta - A) \cos(\theta - A) \end{pmatrix}, \quad (16)$$

which defines the angle offset field as

$$\bar{\Psi} \begin{pmatrix} -Cr \sin^2(\theta - A) \\ -Cr \sin(\theta - A) \cos(\theta - A) \end{pmatrix} \quad (17)$$

As the field is linear in the sense of the application to the angle offset, a compound lens will then have the following tensor field:

$$\bar{\Psi} \begin{pmatrix} -Sr - Cr \sin^2(\theta - A) \\ -Cr \sin(\theta - A) \cos(\theta - A) \end{pmatrix}. \quad (18)$$

Deriving the position of the ray on the retina is therefore simple and can be defined in the same coordinate system as

$$\begin{pmatrix} P_r \\ P_\theta \end{pmatrix} = \begin{pmatrix} r + f_{\text{eye}}(\alpha_r + \Psi_r) \\ f_{\text{eye}}(\alpha_\theta + \Psi_\theta) \end{pmatrix}. \quad (19)$$

In the case of the inverse Shack–Hartman technology, the measurement is differential and entails the overlapping of the rays from the two channels. We assume the two channels in the device are a mirror image of each other with respect to the meridian angle (i.e., one channel corresponds to coordinate r and the other to coordinate $-r$). This would yield the following formulation for the angles (and thus for the position on the screen):

$$\alpha_r = \frac{\Psi_r(-r) - \Psi_r(r)}{2}, \quad (20)$$

$$\alpha_\theta = \frac{\Psi_\theta(-r) - \Psi_\theta(r)}{2}. \quad (21)$$

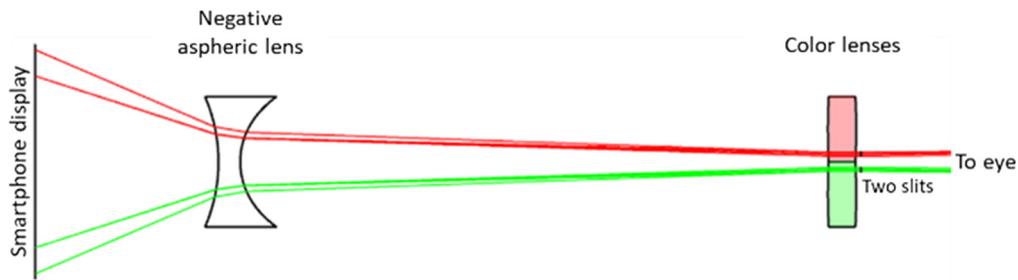


Fig. 10 Basic ray trace of the EyeQue VisionCheck device.

And in the case of a compound lens

$$\alpha_r \propto S + C \sin^2(\theta - A), \quad (22)$$

$$\alpha_\theta \propto C \sin(\theta - A) \cos(\theta - A). \quad (23)$$

1.3 Measurement Device Design

In the case of the VisionCheck device, the optical layout is shown in Fig. 10, corresponding to a single meridian measurement.

The light emanating from the screen goes through an aspheric negative lens that is aimed at correcting distortion in the optical system and provide magnification of the resolution from the screen. As the user adjusts the image on the screen, the smartphone resolution is a limiting factor of the measurement resolution of the refraction values. The VisionCheck device allows use with phones of resolution greater than 250 pixels-per-inch. The light then goes through two color lenses used to separate the light from the screen into two optical channels. The use of chromatic separation is beneficial due to the inherent separation in liquid-crystal displays (LCDs). Furthermore, the chromatic separation allows the users to distinguish between the two distinct colors of the lines drawn on the screen (red and green). The overlapping of the lines could then be easily perceived through the visual cortex as a yellow line. Considering transverse chromatic aberrations in the eye, this approach introduces a misalignment of the visual and chromatic axes. This deficiency is expected to be small as the angles in which the device operates are small. Furthermore, calibration used as the basis for the VisionCheck device operation deals with this problem empirically. Following the color lenses, as light exits the measurement device into the eye, it traverses two slits that provide the required high depth of focus, for performing measurements based on images with users having various refraction errors.

As was shown in Fig. 3, the alignment is only done in one-dimension (1D), which corresponds to the radial direction. The measurement is repeated in nine meridians as shown in Fig. 1. The governing formula for computing the refraction numbers is based on Eq. (22). Though Eq. (22) has only three unknowns, nine meridians are used in the calculation to reduce effects of user error following a proprietary fitting algorithm.

2 Experimental Setup

To assess the device accuracy, an experimental setup was built as shown in Fig. 11.

The experimental setup consisted of a VisionCheck device mounted on a smartphone, and a refraction simulation setup comprised of an iris, a spherical lens, an interchangeable cylindrical lens on a rotation mount, and a camera on a translation stage. The experimental assessment system design followed the concepts in the ISO 10342:2010(E)—Ophthalmic instruments—Eye refractometers standard.¹² The iris was used to reduce spherical aberrations in the image and was set to 4 mm according to the standard. The spherical fixed lens was a 17.5-mm effective focal length (EFL) singlet (Edmund Optics, 38501-INK), similar to the EFL of the human eye. The camera was a color 8MP CMOS detector (Spinel Electronics, UC80MPD), which was mounted on a digital micrometer linear translation stage.

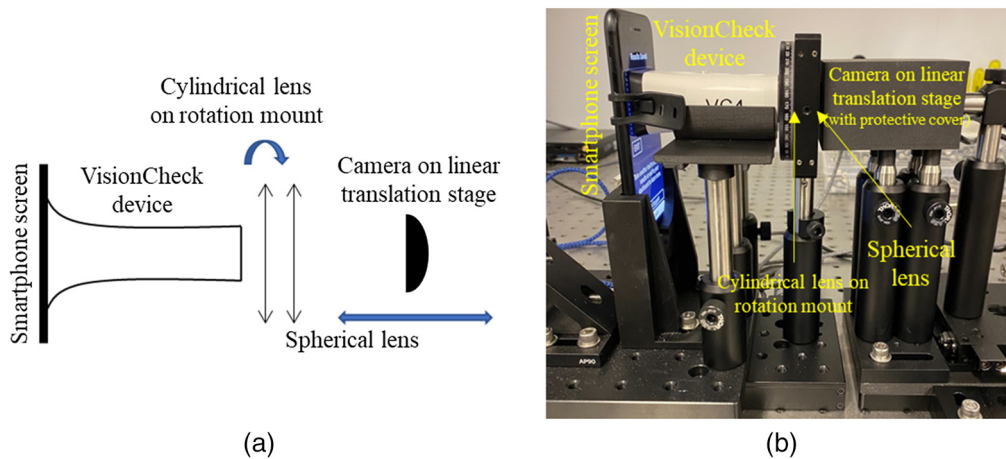


Fig. 11 Experimental setup. (a) Schematic drawing and (b) lab implementation.

The experimental setup preparation entailed mounting the VisionCheck device onto the phone and aligning the optical axis to the experimental assessment system. Mounting the selected cylindrical power lens onto the cylindrical mount and adjusting the angle to the desired axis. Finally, the position of the camera was adjusted to determine the spherical power to be measured.

The measurement was conducted manually by the operator to follow the VisionCheck device standard procedure. The red and green lines were aligned visually through the image viewed on the screen from the camera (Fig. 12).

The measurement was performed for spherical refraction correction between -10 D and $+8$ D in 1D increments, for cylindrical refraction correction between -5 D and 0 D at three different axis values (30 deg, 90 deg, and 170 deg), and for some combinations of the sphere and cylinder values. Additional measurements were taken to assess reproducibility between different VisionCheck devices (three different devices).

As the device is intended for home use by laypeople, optical axis alignment may play an important role in variability of results. An experiment in which the measurement optical setup was aligned in different positions and orientations to the VisionCheck device was conducted. The experiment measured the spherical refraction power with the VisionCheck device as a function of the input refraction power. The measurement was done for powers between -10 D and $+8$ D. The misalignment of the measurement system from the VisionCheck device included positioning offset of 0.5 mm, angular misalignment of 0.75 deg in both horizontal and vertical directions, and an offset along the optical axis of 5 mm. These values were chosen as they represent the edges of the visible field of view through the device (i.e., beyond these the lines are no longer visible).

3 Results

Refraction measurement data were taken from the EyeQue database and converted to power vector notation for analysis.¹³ The power vector notation allows an independent comparison

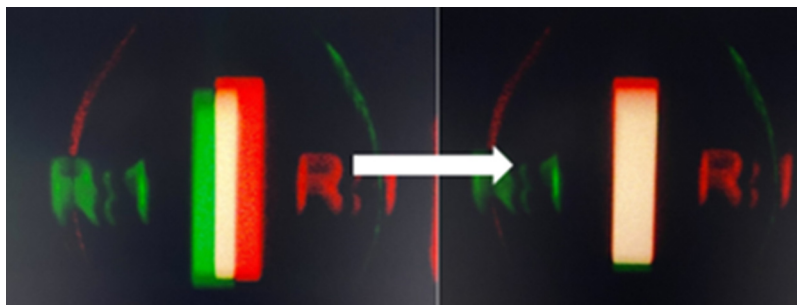


Fig. 12 An example of overlapping the red and green lines.

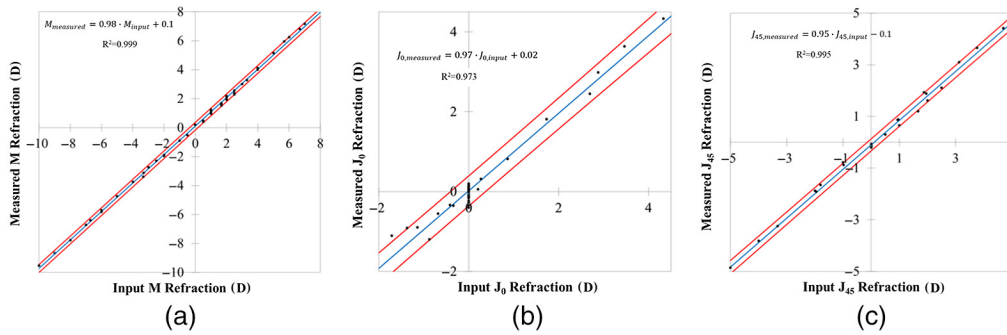


Fig. 13 Refraction measurement linear regression. Black dots represent measured data, blue line the linear fit, and red lines the 95% limits of prediction. (a) M component; (b) J_0 component; and (c) J_{45} component.

of the different components of the refraction data as the sphere, cylinder, and axis notation is not orthogonal. A linear regression model was used to assess the correlation between the input refraction and measured refraction values. The analysis is shown in Fig. 13 and includes a graphical representation of the results, the linear fit, and the 95% prediction limits, along with the linear model formula and the respective R^2 for the M , J_0 , and J_{45} vectors.

It can be seen that the linear models for the refraction power vectors have a slope close to 1: 0.98 for M , 0.97 for J_0 , and 0.95 for J_{45} . The models also show minimal offset (up to 0.1 D) between the input and measurement. The 95% levels of prediction are very close to the linear fit with a single outlier for the negative extreme of the J_0 component. The R^2 correlation coefficients are all above 0.97.

Figure 14 shows the data of the reproducibility measurement. The results show that the standard deviation of the power vectors is 0.1 D for M , 0.1 D for J_0 , and 0.01 D for J_{45} .

Figure 15 shows the results of the pupil alignment experiment. The results show that there is little change due to misalignment of the optical axes of the measurement systems and the VisionCheck. The maximum offset observed was about 0.25 D at the high hyperope end of range. This was expected since the VisionCheck device allows for a very limited field of view, forcing the user to align the device quite closely to the eye's optical axis.

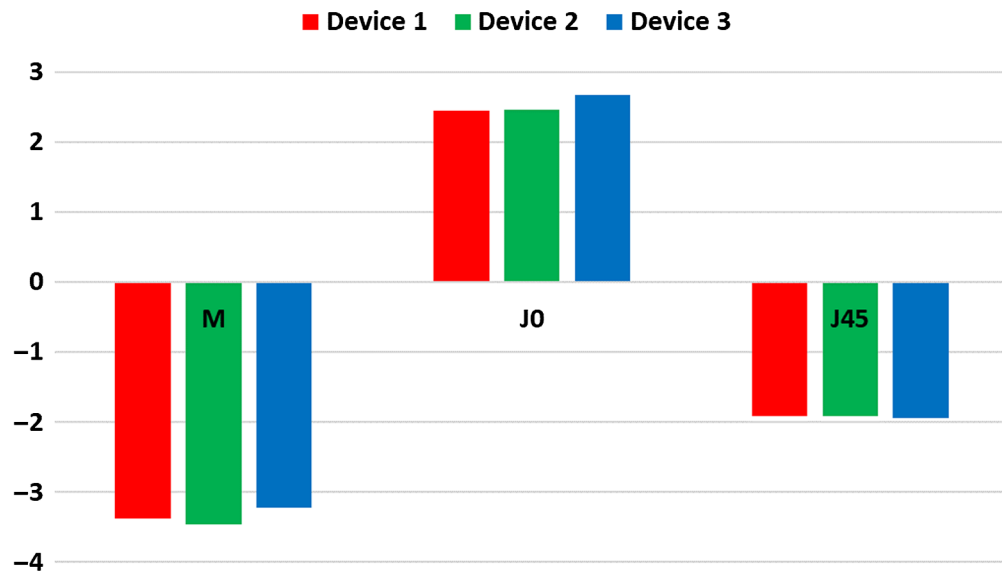


Fig. 14 Reproducibility data of three devices measuring a single target with refraction of S -5D, C -3.33D, and A 63 deg.

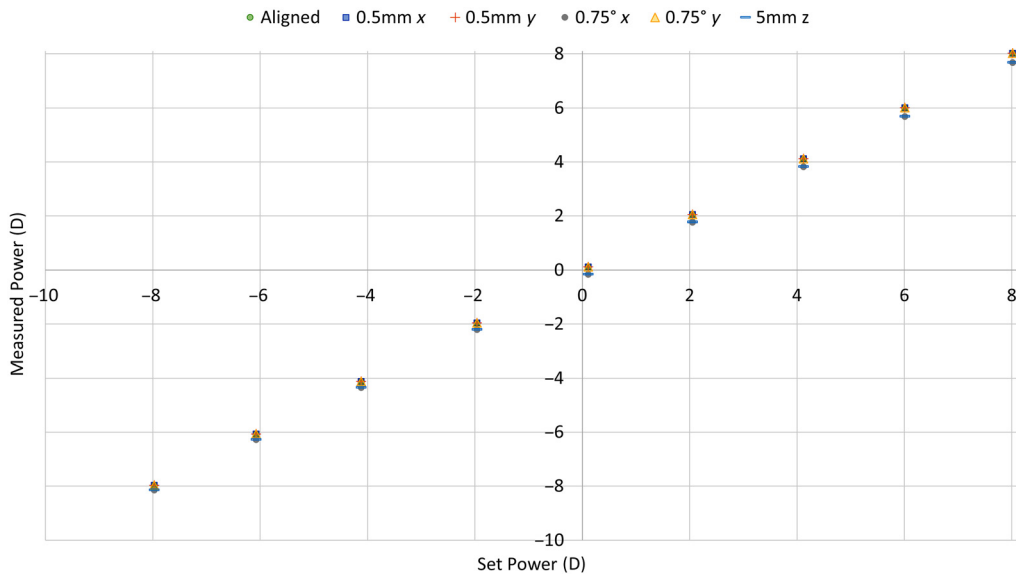


Fig. 15 Misalignment measurement experiment. The horizontal axis represents the measurement system input optical power and the vertical axis represents the measured power. The different colors and shapes represent different misalignment conditions. Most data points overlap per set power.

4 Conclusion

After extensive testing, the EyeQue VisionCheck has been found to provide an accurate measurement of refraction. The range of measurement between -10 D and $+8$ D for spherical refraction and 0 D and -5 D for the cylinder component make the device suitable for optometric measurements for the human eye. The results obtained with the VisionCheck appear to be reproducible across devices and robust to user pupil alignment making it also suitable for at home measurements by laypeople.

References

1. D. Pascolini and S. P. Mariotti, "Global estimates of visual impairment: 2010," *Br. J. Ophthalmol.* **96**(5), 614–618 (2012).
2. World Health Organization (WHO), "Blindness and vision impairment fact sheet" (2018).
3. J. Adler-Milstein, J. Kvedar, and D. Bates, "Telehealth among US hospitals: several factors, including state reimbursement and licensure policies, influence adoption," *Health Aff.* **33**(2), 207–215 (2014).
4. G. Doolittle, A. Spaulding, and A. Williams, "The decreasing cost of telemedicine and telehealth," *Telemed. J. E. Health* **17**, 671–675 (2011).
5. A. Di Cerbo et al., "Narrative review of telemedicine consultation in medical practice," *Patient Prefer. Adherence* **9**, 65–75 (2015).
6. D. A. Hoffman, "Increasing access to care: telehealth during COVID-19," *J. Law Biosci.* **7**(1), Isaa043 (2020).
7. R. Gelburd, "The coronavirus pandemic and the transformation of telehealth," US News and World Report, June 2, 2020. <https://www.usnews.com/news/healthiest-communities/articles/2020-06-02/covid-19-and-the-transformation-of-telehealth> (accessed 8 August 2020).
8. J. Wosik et al., "Telehealth transformation: COVID-19 and the rise of virtual care," *J. Am. Med. Inf. Assoc.* **27**, 957–962 (2020).
9. V. Pamplona et al., "Near eye tool for refractive assessment," US patent 8,783,871 B2 (2014).
10. G. Skolianos et al., "Optical method to assess the refractive properties of an optical system," US patent 10,588,507 B2 (2020).

11. J. Serri, Y. Wang, and N. Sapiens, "Automated personal vision tracker," US patent 2020/0077886 A1 (2020).
12. ISO 10342:2010(E), Ophthalmic instruments—eye refractometers standard.
13. L. N. Thibos, W. Wheeler, and D. Horner, "Power vectors: an application of Fourier analysis to the description and statistical analysis of refractive error," *Optom. Vis. Sci.* **74**(6), 367–375 (1997).

Noam Sapiens is vice president of Science and Technology at EyeQue Corp. He received his PhD in applied physics from the Hebrew University in Jerusalem, Israel. He has over 25 years of experience leading technology development in various field of optics. He is a member of SPIE.

Patrick O'Neal is an optical engineer at EyeQue Corp. He received his MS degree in optical sciences from the University of Arizona. He is a member of SPIE.